Enlarged Plasma Ablations in Microwave-Enhanced Laser-Induced Breakdown Spectroscopy with Coaxial Multifiber Arrays

Y. Ikeda* and J.K. Soriano

i-Lab., Inc. KIBC #213, 5-5-2 Minotima-Minami Kobe, 65-0047 Japan
* Correspondent author: yuji@i-lab.net

Keywords: Microwave, Ignition, Plasma Temperature, Volumetric Plasma, High Speed Images

ABSTRACT

This study comprises a comprehensive investigation of the enhancement of laser-induced breakdown spectroscopy (LIBS) using multifiber array configurations and microwave (MW) enhancement. We demonstrated a significant increase in both the emission intensity and Signal-to-Noise Ratio (SNR) through the integration of a six-multifiber setup, resulting in a six-fold increase in broadband emissions. The introduction of MW further augmented this enhancement, exhibiting a two to three orders of magnitude increase in emissions. Remarkably, the combined approach of multifiber LIBS and MW enhancement resulted in a dramatic 2000-time improvement in emission signals. Concurrently, the SNR was enhanced by two to three orders of magnitude. These advancements have opened new avenues for expanding the limits of detection in analytical applications, which is the focus of our ongoing investigation. Our findings have significant implications for various industries including environmental monitoring, materials science, and biomedical research.

1. Introduction

Laser-Induced Breakdown Spectroscopy (LIBS) is widely used for elemental analysis because it enables rapid testing(Qi, Zhang, Tang, & Li, 2018), requires minimal sample preparation(Fichet, Tabarant, Salle, & Gautier, 2006), offers the ability to conduct remote assessments(Rohwetter et al., 2004), and provides real-time results(H. Li, Mazzei, Wallis, Davari, & Wexler, 2021). LIBS involves directing a high-powered laser onto a sample, resulting in breakdown due to multiphoton absorption and inverse bremsstrahlung photoionization(Thakur & Singh, 2020). This action triggers the formation of plasma, and the emitted light reveals the elements within the sample(Rai & Thakur, 2020).

Along with these advantages, LIBS also has some limitations. One challenge is the rapidly fluctuating and exceedingly small plasma shape (Kawahara, Beduneau, Nakayama, Tomita, & Ikeda, 2007)accompanied by an exceptionally short duration of stable plasma for elemental analysis(Ikeda, Soriano, Kawahara, & Wakaida, 2022). Strategies to mitigate these issues include the use of beam shaping and incorporating noble gas environments to control the impact of ablation(Khumaeni, Akaoka, Miyabe, & Wakaida, 2021), and the employment of various plasma stabilization methods such as spatial and magnetic confinement(Guo et al., 2011; C. Li et al., 2014a, 2014b), dual-pulse breakdown(Pedarnig et al., 2014; Zhang et al., 2022), and microwave (MW)-assisted breakdown(Hayashi et al., 2017; Ikeda, Hirata, Soriano, & Wakaida, 2022; Ikeda, Ofosu, & Wakaida, 2020; Khumaeni, Miyabe, Akaoka, & Wakaida, 2017; Le, Padala, Nishiyama, & Ikeda, 2017; Liu, Baudelet, & Richardson, 2010; Liu, Bousquet, Baudelet, & Richardson, 2012; Al Shuaili, Al Hadhrami, Wakil, & Alwahabi, 2019; Jan Viljanen, Sun, & Alwahabi, 2016).

Among these mitigation strategies, MW-assisted breakdown is a promising approach. It demonstrated considerable success in increasing spatial stability over longer periods(Ikeda, Soriano, Kawahara, et al., 2022), thereby enhancing the reliability of the elemental analysis(Chen, Iqbal, Wall, Fumeaux, & Alwahabi, 2017; Ikeda & Soriano, 2022; Ikeda, Soriano, Akaoka, & Wakaida, 2023b; Ikeda, Soriano, & Wakaida, 2022; Ikeda Yuji, Soriano Joey Kim, & Wakaida Ikuo, 2023; Khumaeni, Motonobu, Katsuaki, Masabumi, & Ikuo, 2013; Tang et al., 2018; J. Viljanen, Zhao, Zhang, Toivonen, & Alwahabi, 2018; Wolk et al., 2013). Plasma expansion by MW resulted in two-to-three degrees of magnitude increase compared with standard LIBS(Ikeda, Soriano, Ohba, & Wakaida, 2023d). This expansion is sustained over time, increasing the spatial stability and extending the analysis window. Plasma expansion exhibits a direct correlation with the notion of absorbed MW(Ikeda, Soriano, & Wakaida, 2023a), which is a consequence of the impedance-matching process between the MW source and laser-induced plasma. This impedance is initially high but further improves as the electron density in the laser-induced plasma decreases. The stable period of plasma formation increased from a typical nanosecond in standard LIBS to milliseconds, even at a modest laser energy of 2 mJ. This is a direct consequence of the prolonged plasma lifetimes observed for metals (stainless steel and zirconium metal) (Ruas, Matsumoto, Ohba, Akaoka, & Wakaida, 2017) and oxides (alumina oxide, gadolinium oxide, zirconium oxide, and uranium oxide)(Ikeda, Soriano, & Wakaida, 2023a; Nakanishi, Saeki, Wakaida, & Ohba, 2020; Tampo et al., 2014). The incorporation of MW extends the plasma lifetime beyond that of standard LIBS by promoting the re-excitation of neutrals and ions within the laser-induced plasma(Ikeda, Soriano, Akaoka, et al., 2023b).

Previously, we successfully applied Microwave-enhanced Laser-induced Breakdown Spectroscopy (MWE-LIBS) to various materials(Ikeda & Soriano, 2023; Ikeda, Soriano, & Wakaida, 2023b). This led to significant improvements in the signal-to-noise ratios (SNR) for alumina(Ikeda,

Soriano, Kawahara, et al., 2022), lead(Ikeda, Soriano, & Wakaida, 2022), stainless steel(Ikeda, Soriano, & Wakaida, 2022), zirconium metal, and oxide(Ikeda, Soriano, & Wakaida, 2023b). We have also extended the Limit of Detection (LOD) for gadolinium (Ikeda, Soriano, Ohba, & Wakaida, 2023e)and have seen numerous enhancements in isotope analysis for uranium(Ikeda, Soriano, Ohba, & Ikuo, 2023a), as the MWs help stabilize the emission.

Although MWE-LIBS presents numerous advantages, it is not without limitations such as elevated background noise (Ikeda, Soriano, & Wakaida, 2023b) and minimal impact on mitigating matrix effects or self-absorption(Karino et al., 2023). In the context of single-point plasma emission collection, background noise tends to increase owing to the accumulation of collected emissions. However, when employing multiple collection points and compressing emissions into a single fiber, background noise can be controlled. This challenge is the focus of our research objectives for advancing emission collection in MWE-LIBS.

Figure 1 illustrates a critical development: a 20-fold volume expansion of Al plasma under MW irradiation. To capitalize on this, our research focused on enhancing large-area emission collection and optimizing the SNR. By deploying multipliers in large-area emission collection, we significantly amplified the detection capabilities of MWE-LIBS. This innovation serves as a pivotal driver for breakthroughs in the analysis of Al alloys. The urgency for these advancements is fueled by the increasing demand for refined identification methods for recycling Al alloys.

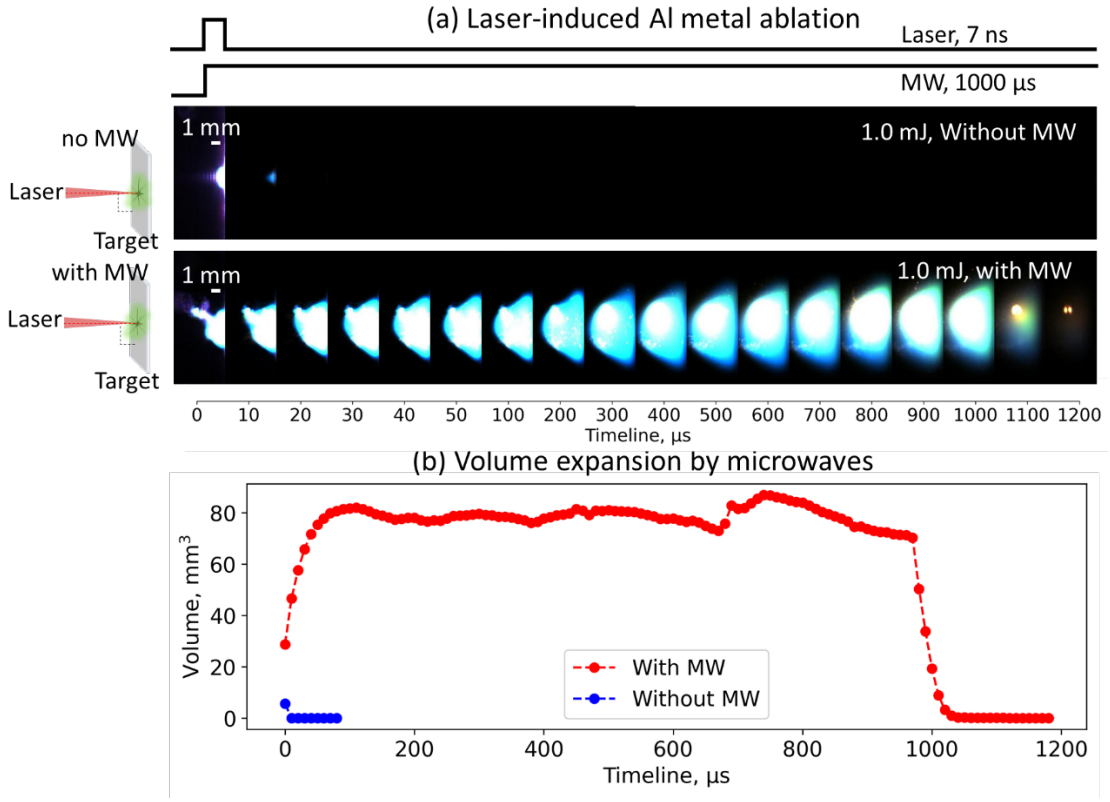

Figure. 1 (a) Enlarged plasma emission of laser ablated Al plasma by MW and their corresponding (b) approximated volume (Ikeda, Soriano, Kawahara, et al., 2022).

2. Methodology

Figure 2 shows the experimental setup of the MWE-LIBS with multifiber emission collection. The fiber and optics configuration serves a dual purpose: a 1053 nm laser (Q1, Quantum Light Instruments, Lithuania) is propagated through the central fiber of a multifiber bundle (RP20 and FT200UMT, Thorlabs, NJ), while the surrounding fibers are designated for the collection of plasma emissions, which are enlarged via MW facilitation. Emissions captured by these multiple fibers are then funneled into a single 200 μm diameter fiber. This channeling is executed using a series of collimating and focusing lenses developed in-house and specifically designed to optimize the process of emission collection.

The MWe system is operated at a frequency of 2.45 GHz, power output of 1 kW, and duration of 1 ms. The energy from the MW was transmitted through a helical antenna. This setup was carefully engineered to provide precise control over the emission enlargement process, thereby enhancing the overall efficacy of MWE-LIBS.

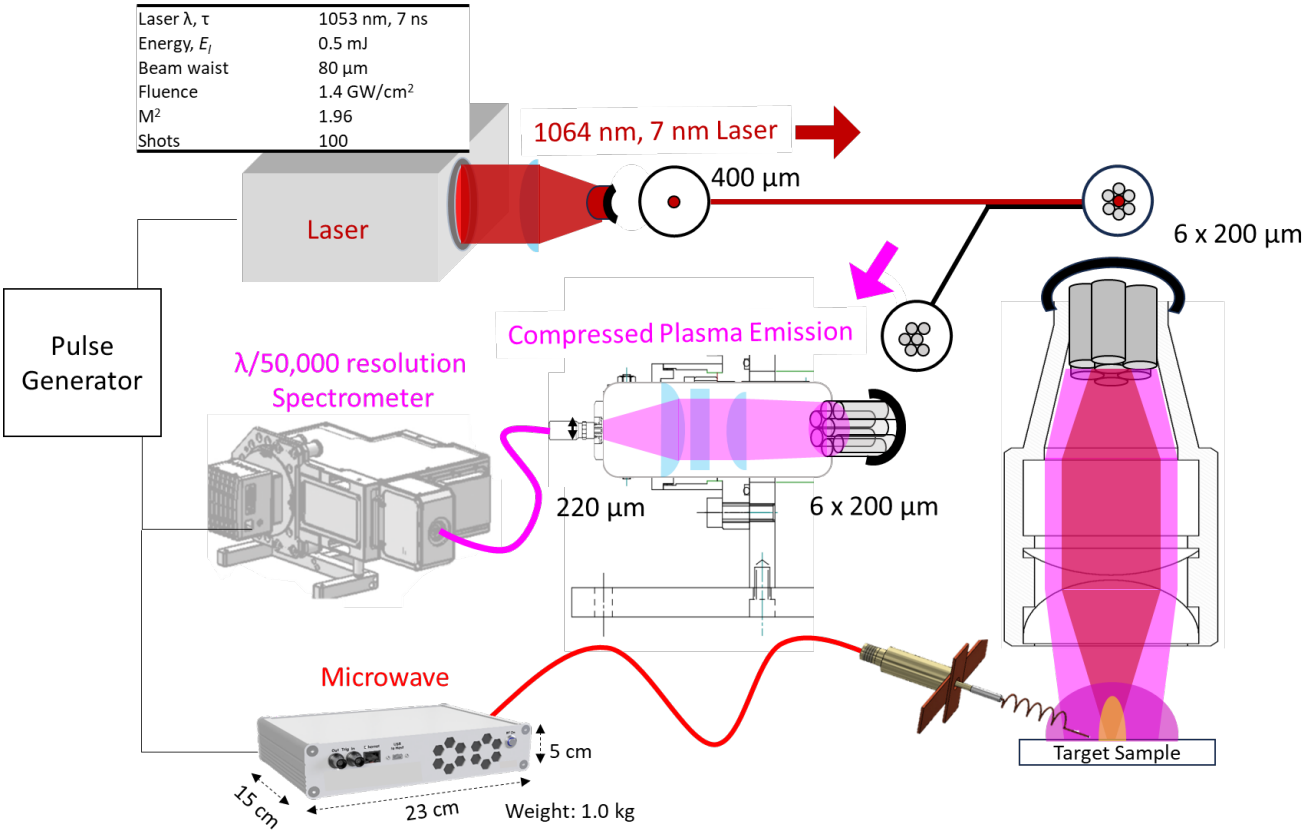

Figure. 2 Multifiber configuration in MWE LIBS.

Plasma emissions were analyzed using an echelle spectrometer (EMU-120/65, Catalina Scientific, AZ, USA). The Catalina spectrometer was configured with a diffraction grating having a specific groove density, providing a spectral resolution of λ/15,000. Emission signals are collected with a gate width of 1000 μs and a gate delay of 0.5 μs to optimize the SNR. The exposure time for each measurement was set to 1.0 ms. The spectrometer was calibrated using a standard spectral lamp to ensure the accuracy of the wavelength assignments. The fiber used for collecting emissions has a core diameter of 600 μm, facilitating efficient light collection. Furthermore, the focusing lens with a focal length of 25 mm also contributed to signal optimization. All parameters were carefully selected to maximize the collection of plasma emissions while maintaining controlled background noise levels.

Figure 3 illustrates the essential functions of multifiber systems in the realm of emission collection. Experimental data derived from MW-amplified air plasma indicated an enlargement factor as high as 100-fold. In specific numerical terms, this translates into a prospective expansion of the plasma cross-sectional area from an initial value of 0.013 mm² to an approximate value of 1 mm². This expansion is achieved through the utilization of a 200 μm fiber, augmented by specialized focusing optics developed in-house.

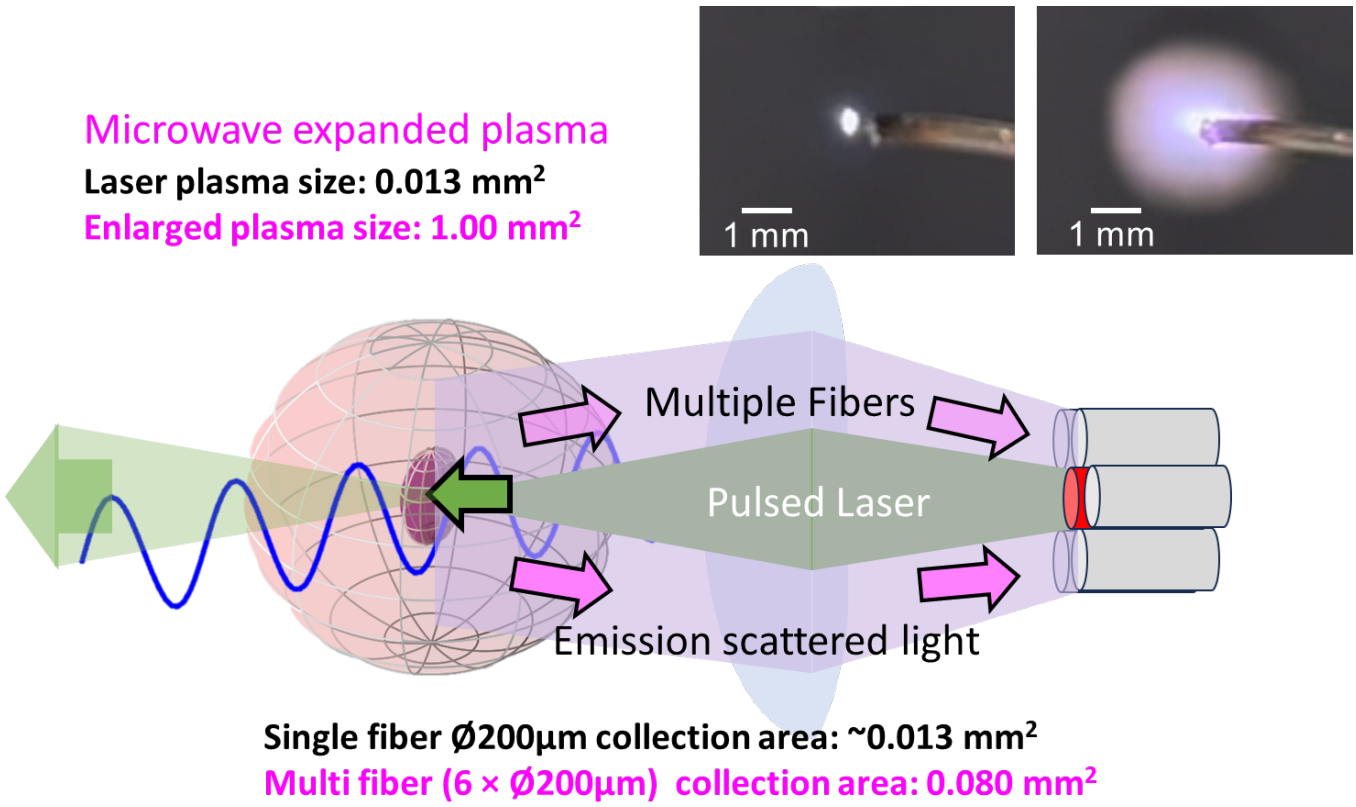

Figure. 3 Illustration of enlarged area collection using multifiber LIBS. The plasma size is based on the reported data in reference (Ikeda, Soriano, Ohba, & Ikuo, 2023c).

The limitations of single-fiber collection methods are evident when viewed in this context; a single fiber can capture only a minimal portion of the total emission surface area. Conversely, the multifiber methodology allows emissions collection over an expansively large surface area. This not only enhances the data quality but also serves to optimize the utility of MWE-LIBS. Consequently, the use of a multifiber system has emerged as both a practical and effective strategy for capitalizing on the inherent advantages of this advanced spectroscopic technique.

The primary objective of our research is to collect large-area emission data to substantially improve the SNR. In addition, we utilized strict noise control and management protocols to maintain the data quality. As demonstrated in Figure 4, preliminary tests using multifiber systems on the Al I line showed a more than two-fold increase in emission compared with a single-fiber setup. However, this increase was accompanied by an increase in the background noise.

This dual outcome lays the groundwork for current research efforts. The focus now extends to investigating methods for controlling or potentially reducing this elevated background noise without compromising enhanced emission rates. Ultimately, our targeted approach aims to optimize the integration of multifiber components into MWE-LIBS, with the ultimate goal of achieving significant advancements in elemental analysis.

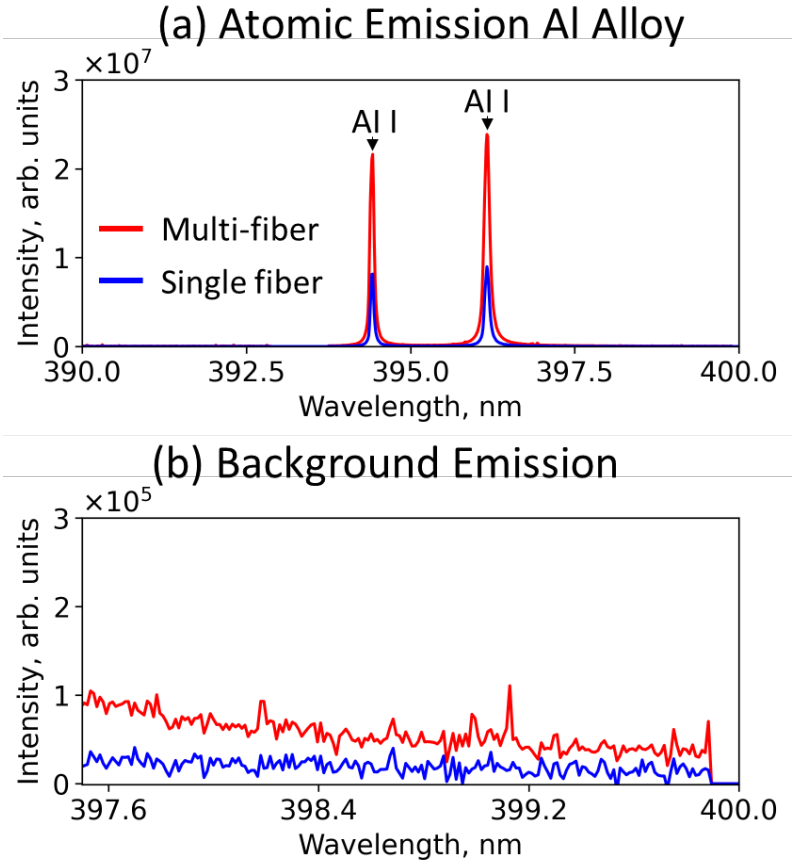

Figure. 4 (a) Atomic emission of Al Alloy and (b) the background emission level without microwaves.

3. Results

Figure 5 offers compelling evidence for the efficacy of multifiber configurations in LIBS by comparing it with the single-fiber setup. Notably, the area under the broadband emission curve measured across the wavelength range of 400–800 nm experienced a six-fold increase when a multifiber configuration was used instead of a single fiber. Additionally, Figure 5 highlights a specific xenon emission line at 479.3 nm, where a four-fold increase in the intensity was observed. This further substantiates the advantages of using the multifiber approach in LIBS applications.

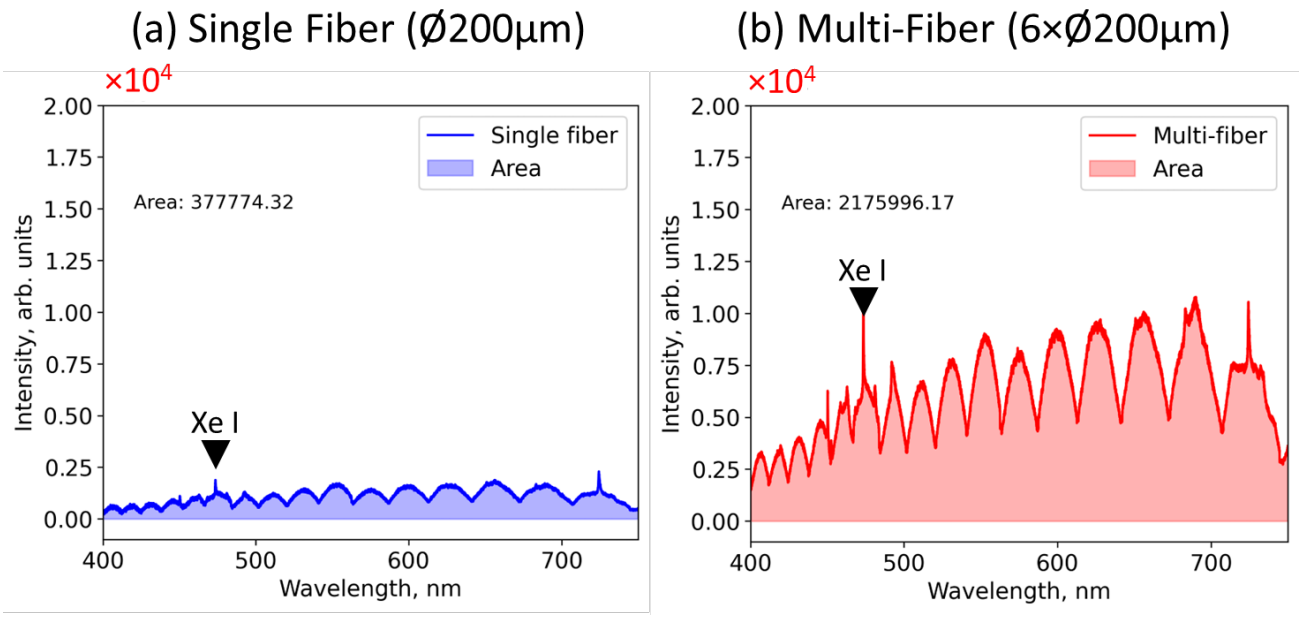

Figure. 5 Continuum emission from Xe lamp collected by a (a) single fiber versus (b) multiple fibers compressed into one single fiber. Fiber core: 200 μm, 0.22 NA. Outer fiber: 200 μm, 0.22 NA. Spectrometer resolution: $\lambda/30{,}000$. Temporal settings: Exposure = 1 ms, Intensifier gain = 3500.

In the context of practical applications, experiments were conducted on an aluminum alloy target to assess the role of MW in enhancing emissions in both single- and multifiber configurations of LIBS.

Figure 6a shows the emissions for conditions with and without MW using only a single fiber. The laser power used was 1 mJ, and the four highest elemental compositions of the Al alloy were labeled as Al I, Fe I, Mn I, and Cu I. Figure 6b on the other hand shows the effects of MW enhancements on multifiber configurations. The data reveal that while MWs enhance emission in both configurations, the magnitude of this enhancement is markedly higher when employing a multifiber setup. These findings were obtained under specific experimental conditions, with an exposure time of 1 ms and a gate delay of 1 μs, thereby underscoring the efficacy of multifiber configurations for emission signal amplification.

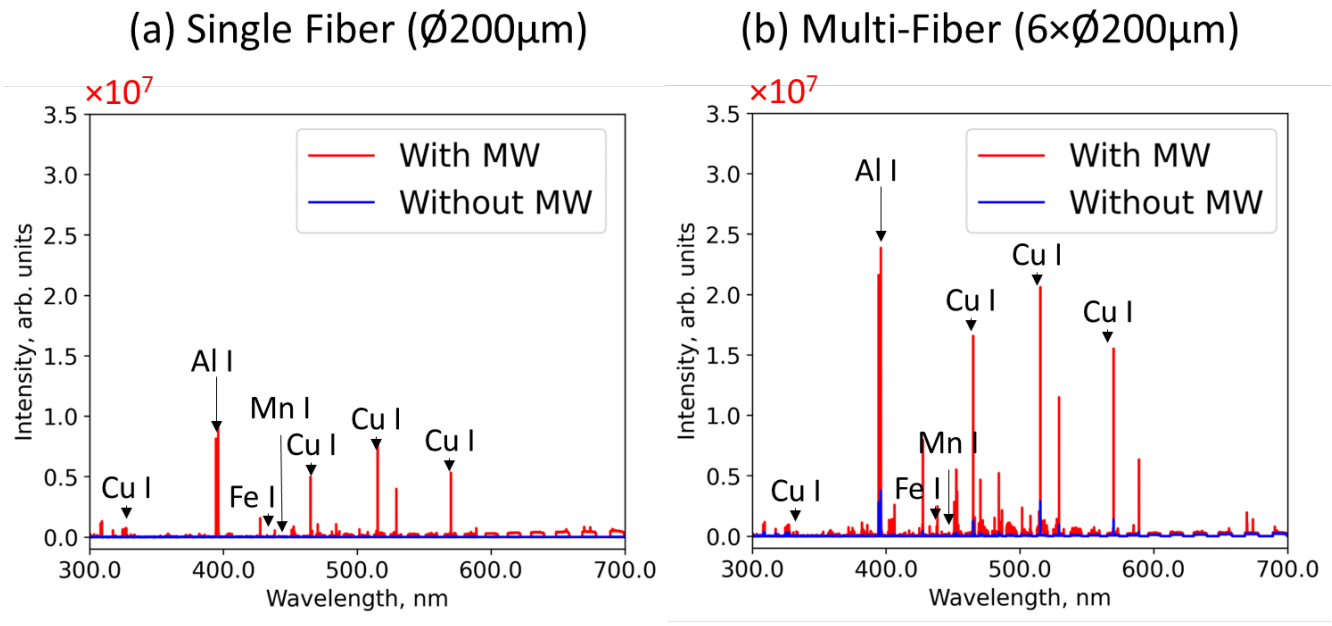

Figure. 6 Comparative emission collection in (a) single-fiber LIBS and (b) multifiber LIBS under microwave (MW) and non-MW conditions. Laser specs: λ = 1053 nm, τ = 7 ns, E_l = 0.5 mJ, Fluence = 1.4 GW/cm^2, M^2 = 1.96, 100 shots. Fiber core: 200 µm, 0.22 NA. Outer fiber: 200 µm, 0.22 NA. Spectrometer resolution: λ/30,000. Temporal settings: Exposure = 1 ms, Gate delay = 1 μs, Intensifier gain = 3500.

Upon closer examination of the emission spectrum between 393.5 and 397 nm, shown in Figure 7, distinct peaks corresponding to enhanced emissions of Aluminum I lines at 394 and 396 nm became evident. These peaks serve as notable indicators of the effectiveness of our experimental approach in enhancing the emission signals.

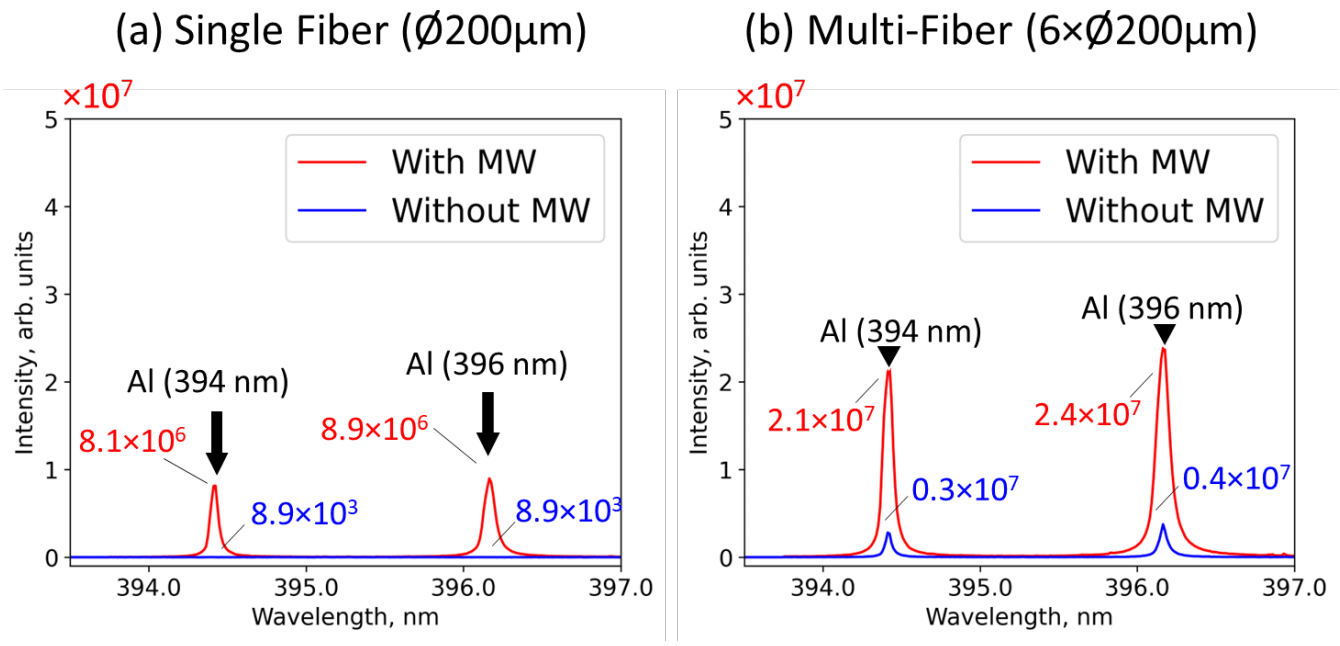

Figure. 7 Comparison between atomic emission of Al I line in (a) single-fiber LIBS and (b) multifiber LIBS under microwave (MW) and non-MW conditions.

Figure 8 shows a comparative analysis of the Al I atomic emissions under four specific experimental setups: multifiber LIBS with MW assistance, multifiber LIBS without MW assistance, single-fiber LIBS with MW assistance, and single-fiber LIBS without MW assistance. Notably, the data indicate that MW conditions enhance the emission intensities in both single- and multifiber configurations compared with their non-MW-enhanced counterparts.

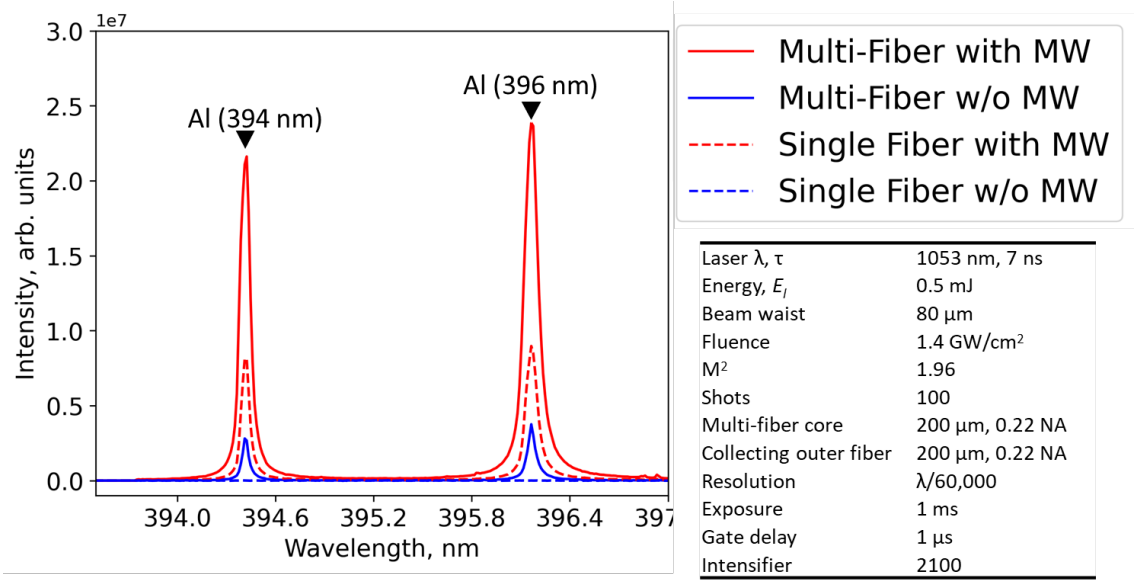

Figure. 8 Comparative analysis of Al I atomic emissions in four experimental setups: multifiber LIBS with and without microwaves (MW), and single-fiber LIBS with and without MW.

Figure 9 illustrates the impact of varying gate delay times on the Al emissions in multifiber LIBS. Central to this investigation was the role of time integration in the collection of emissions examined across different gate delay settings. These data highlighted the role of MW in maintaining elevated emission levels over time. Irrespective of the gate delay, the MW-enhanced conditions consistently yielded higher emission intensities than those achieved without MW assistance.

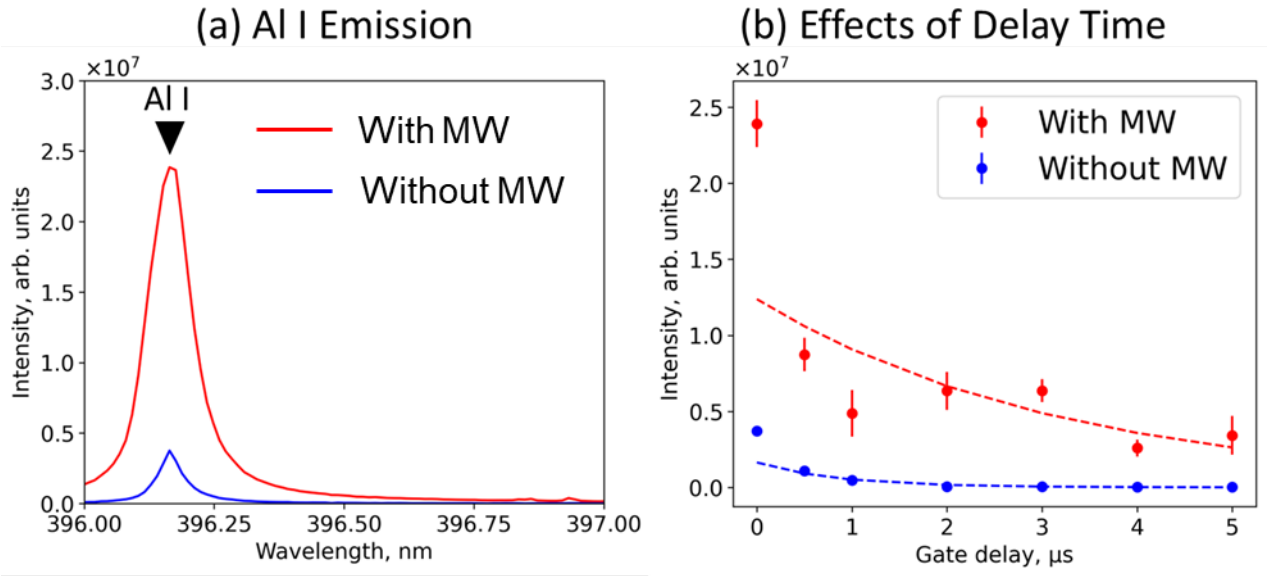

Figure. 9 Impact of gate delay times on Al I emissions, highlighting the role of time integration and microwave (MW) enhancement. MW conditions consistently yield higher emission intensities across all gate delay settings.

Figure 10 shows a comparative analysis of the SNR and intensity ratio with and without MW enhancement. Remarkably, the graph reveals that both metrics benefit from MW exposure, exhibiting an increasing trend as the gate delay settings are extended. This demonstrates that MW assistance not only elevates the SNR but also improves the intensity ratio, affirming its value in enhancing the LIBS performance, particularly at longer gate delays.

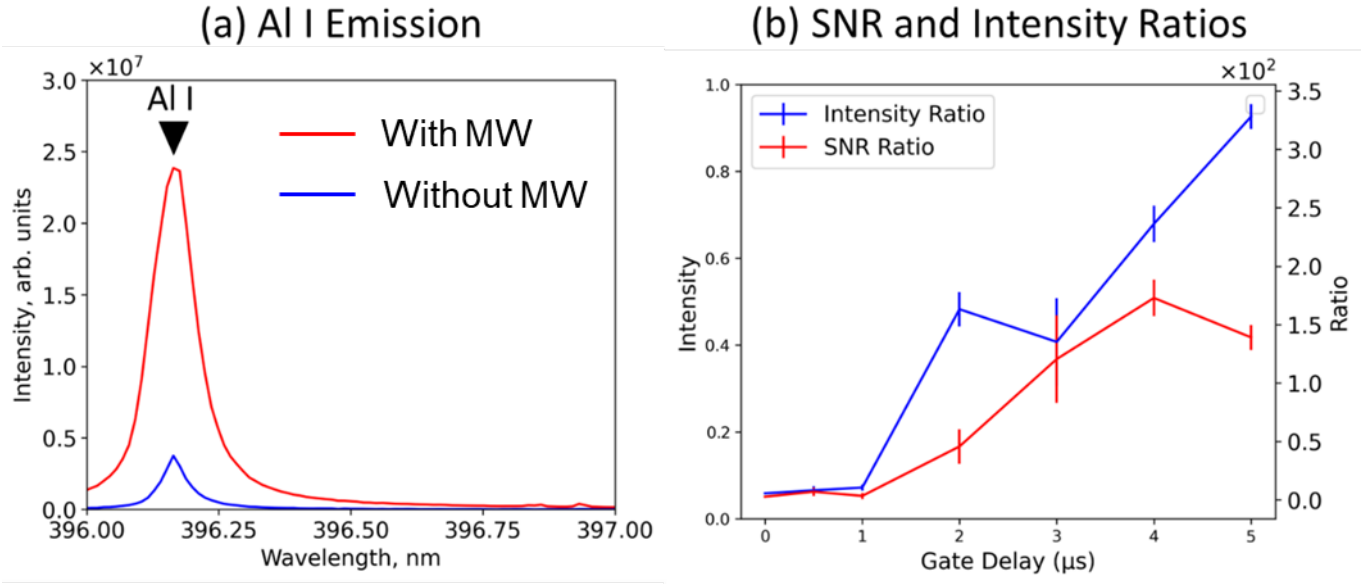

Figure. 10 Comparison of SNR and intensity ratio with and without MW enhancement across varying gate delays. MW consistently improve both metrics, especially at longer gate delays.

Figure 11 compare the intensity of spectral lines of aluminum (Al I) at different energy levels, both with and without the application of microwaves (MW). In both graphs, the X-axis represents the energy levels in electron volts (eV), while the Y-axis shows the intensity in units of ×107\times 10^7×107. The red lines and dots indicate the data points and trend lines with MW, whereas the blue lines and dots represent the data without MW.

For sigle fibers, there is a notable peak in intensity at the 4.0 eV energy level when MW is applied, indicated by a maximum Intensity Enhancement Factor (IEF) of 400. This significant increase in intensity with MW at the 4.0 eV level contrasts sharply with the low intensity observed without MW. For other energy levels, such as 7.6 eV and 3.1 eV, the intensity remains negligible in both scenarios.

Similarly, multifiber arrays also shows an increase in intensity at the 4.0 eV energy level with MW, but the enhancement is less pronounced, with a maximum IEF of 7.5. As with the left graph, the intensity at other energy levels remains low regardless of MW application. The energy levels and their corresponding wavelengths are as follows: Al I (206 nm, 7.6 eV), Al I (208 nm, 4.0 eV), Al I (209 nm, 4.0 eV), Al I (294 nm, 3.1 eV), and Al I (296 nm, 3.1 eV).

Both graphs highlight a significant increase in intensity at the 4.0 eV energy level when MW is applied, with single fiber showing a higher enhancement factor compared to the multifiber. The intensity for other energy levels remains negligible in both graphs, demonstrating the specific effect of MW on the 4.0 eV transition in aluminum.

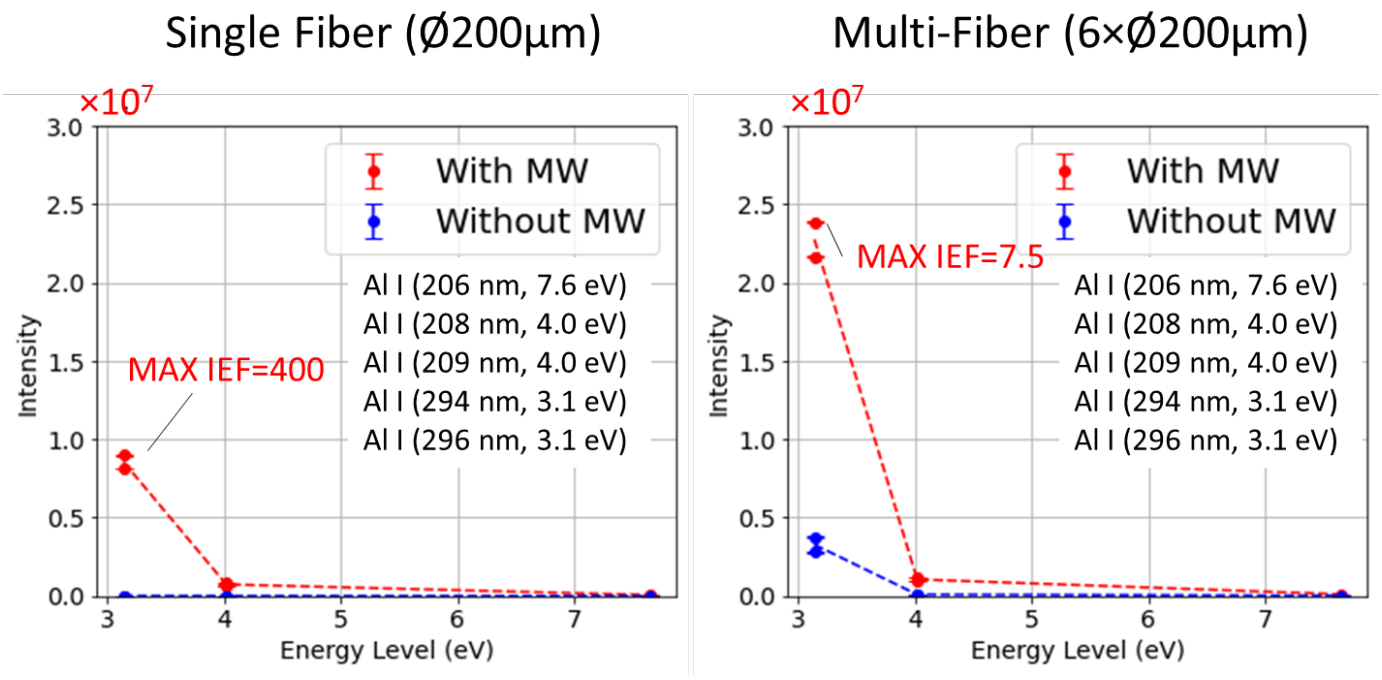

Figure. 11 Comparison of spectral line intensities of aluminum (Al I) at various energy levels with and without the application of microwaves (MW).

Figure 12 compares the SNR of aluminum (Al I) spectral lines at different energy levels, both with and without the application of microwaves (MW). In both graphs, the X-axis represents the energy levels in electron volts (eV), while the Y-axis shows the SNR on a logarithmic scale ranging from 10010^0100 to 10610^6106. The red lines and dots indicate the data points and trend lines with MW, whereas the blue lines and dots represent the data without MW.

For single fibers, there is a notable increase in SNR with MW at the 4.0 eV energy level, where the SNR reaches approximately 10310^3103, compared to an SNR around 10110^1101 without MW. For other energy levels, such as 7.6 eV and 3.1 eV, the SNR remains low in both scenarios, with a more noticeable decrease in SNR with MW.

Similarly, multifiber arrays also shows a peak in SNR with MW at the 4.0 eV energy level, but the enhancement is slightly less pronounced compared to the left graph. The SNR for other energy levels, such as 7.6 eV and 3.1 eV, remains low in both cases. The overall trend in both graphs shows a decrease in SNR with MW across the energy levels, except for the significant peak at 4.0 eV.

Single and multifiber arrrays highlight a significant increase in SNR at the 4.0 eV energy level when MW is applied, with the left graph showing a higher SNR compared to the right graph. The SNR for other energy levels remains low in both graphs, demonstrating the specific enhancement effect of MW on the 4.0 eV transition in aluminum. The energy levels and their corresponding

wavelengths are: Al I (206 nm, 7.6 eV), Al I (208 nm, 4.0 eV), Al I (209 nm, 4.0 eV), Al I (294 nm, 3.1 eV), and Al I (296 nm, 3.1 eV).

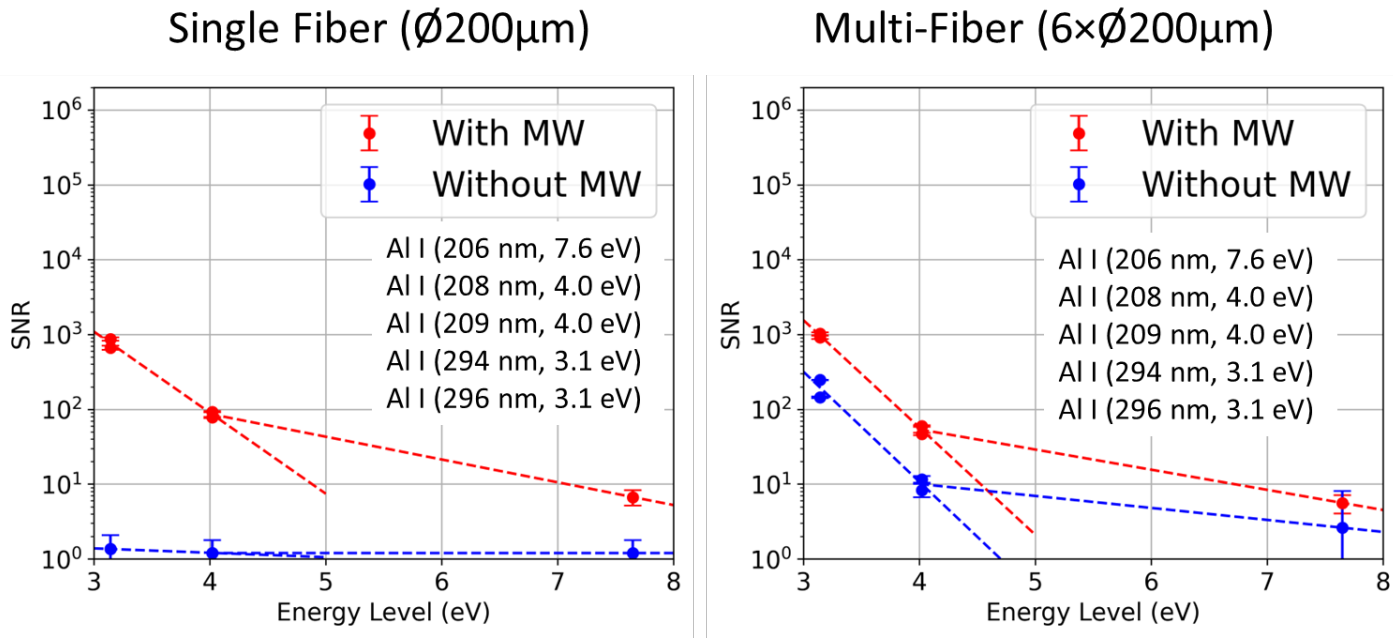

Figure. 12 Comparison of the Signal-to-Noise Ratio (SNR) of aluminum (Al I) spectral lines at various energy levels with and without the application of microwaves (MW).

The Limit of Detection (LOD) measurements of Al I [394] in multifiber Laser-Induced Breakdown Spectroscopy (LIBS) with microwaves are shown in Figure 13. This figure illustrates the enhancement effect of microwaves on the intensity of Al I [394] emissions at different aluminum concentrations. The red data points and trend line represent measurements taken with microwaves, showing a significantly higher intensity compared to the blue data points and trend line, which represent measurements without microwaves.

Microwave-assisted LIBS can increase the Signal-to-Noise Ratio (SNR) because the background noise is not enhanced by microwaves, which only enhance the ablation plasma. In contrast, increasing the number of receiving fibers increases scattering locations, but the plasma generation characteristics with and without microwaves do not change for multiple fibers.

However, there is a tradeoff when extending the LOD; the standard deviation also increases. A significant tradeoff is observed with the increased Intensity Enhancement Factor (IEF) and SNR due to the much higher light intensity. This higher intensity includes light from different scattering locations, leading to higher noise levels. Our conclusions demonstrated that microwaves can enhance IEF and SNR, as well as the number of fibers used. However, multiple fibers cannot improve the LOD and achieve smaller standard deviations because of the multiple scattered locations.

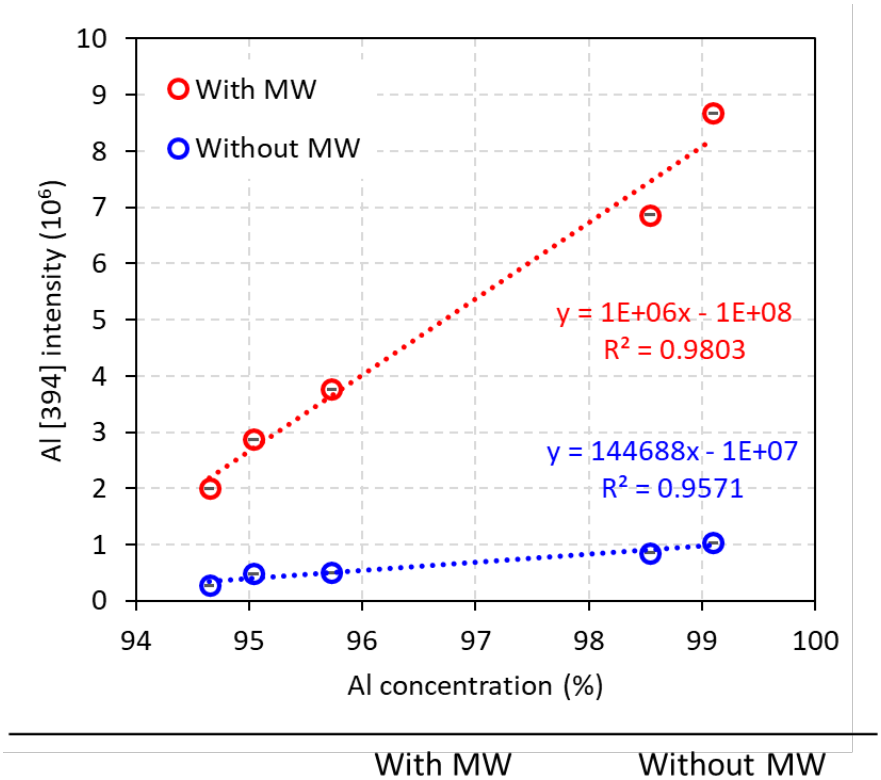

	With MW	Without MW
Slope	1.00E+06	1.40E+05
Standard Deviation	4293	1216
LOD	0.013 %	0.025 %

Figure. 13 Limit of Detection (LOD) measurements of Al I [394] in multifiber Laser-Induced Breakdown Spectroscopy (LIBS) with microwaves. The red data points indicate measurements with microwaves, showing a significantly higher intensity compared to the blue data points without microwaves. The trend lines illustrate the relationship between aluminum concentration (%) and Al I [394] intensity, with microwaves significantly enhancing the signal.

4. Discussions

Our research primarily examined two key advances to enhance the performance of LIBS: the integration of multifiber setup and the application of MW enhancement. Results indicated a substantial increase in both the emitted signal intensity and SNR when transitioning from single-fiber to multifiber configurations, as demonstrated in Figure 14. Specifically, the SNR improved by over a factor of 1000, owing to a more than 2000-fold enhancement in intensity facilitated by microwaves. In the absence of microwaves, we still observed a hundred-fold increase in both SNR and intensity. The enhancement is largely attributed to the higher light-collection efficiency and more comprehensive emission capture offered by the multifiber configuration.

However, the multifiber setup is not without its challenges. The focus of the outer collecting fibers is constrained to the periphery of the central fiber that transmits the laser light. This limitation is especially problematic in single-fiber systems, where focusing the collecting fiber onto the narrow plasma region is not feasible. Fortunately, the use of microwaves alleviates this issue by causing the plasma to expand, thereby facilitating more effective light collection even in single-fiber setups.

In summary, incorporating microwaves into both single and multifiber configurations led to further enhancements in emitted intensities. The synergistic effect of MW and multifiber integration substantially boosts signal strength, thus elevating the SNR. As our ongoing research aims to extend the detection limits for elemental analysis, these advancements offer promising prospects for applications across a diverse range of materials. Future studies will focus on quantifying the impact of the multifiber setup on detection limits.

To summarize, the SNR and IEF can be enhanced up to 2000-fold using microwaes using both types of fibers. In multifiber setups, this results in the collection of much more light, and the quality is already at par with single fibers + microwaves. Improvement through microwave also significantly increases light scattering, leading to higher noise levels and larger standard deviations. As a consequence, the LOD is extended by 50% which is much higher than expected.

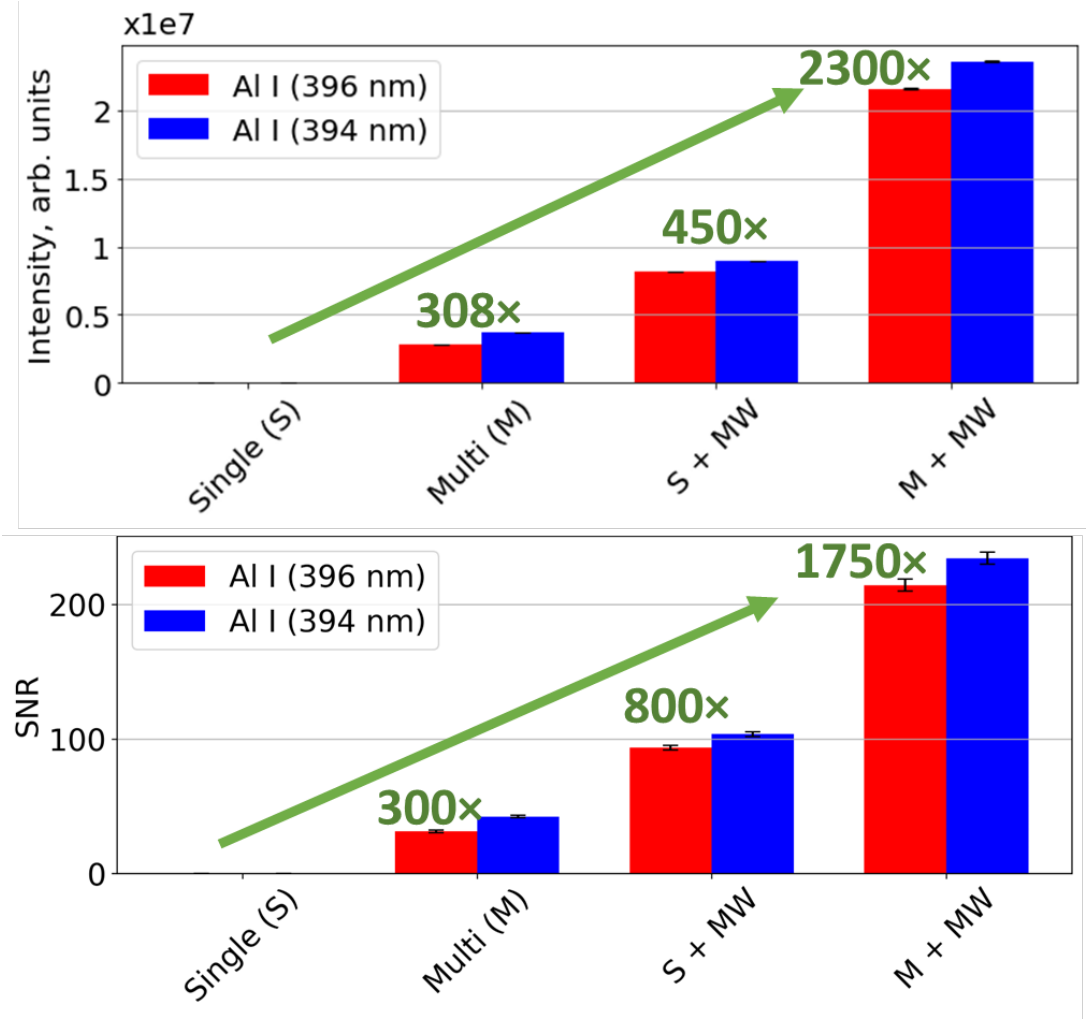

Figure. 14 Enhanced intensity and SNR in multifiber configurations compared to single-fiber setups, attributed to improved light collection and broader emission capture.

5. Conclusions

In conclusion, our study demonstrated significant advancements in the use of multifiber configurations to increase both the intensity and SNR in LIBS. Specifically, we observed a six-fold increase in broadband emissions solely through the incorporation of a six-multifiber setup. Furthermore, the introduction of MW contributed to a six-fold increase in emission intensities. Remarkably, when combining both multifiber integration and MW enhancement, we achieved over 2000 times enhancement of the emitted signals. This led to an improvement in the SNR by three orders of magnitude. One of our primary objectives is to extend LOD, and our ongoing research is aimed at optimizing and furthering these promising technologies.

References

Chen, S. J., Iqbal, A., Wall, M., Fumeaux, C., & Alwahabi, Z. T. (2017). Design and application of near-field applicators for efficient microwave-assisted laser-induced breakdown spectroscopy. *Journal of Analytical Atomic Spectrometry*, *32*(8), 1508–1518. Royal Society of Chemistry.

Fichet, P., Tabarant, M., Salle, B., & Gautier, C. (2006). Comparisons between LIBS and ICP/OES. *Analytical and Bioanalytical Chemistry* (Vol. 385, pp. 338–344).

Guo, L. B., Li, C. M., Hu, W., Zhou, Y. S., Zhang, B. Y., Cai, Z. X., Zeng, X. Y., et al. (2011). Plasma confinement by hemispherical cavity in laser-induced breakdown spectroscopy. *Applied Physics Letters*, *98*(13).

Hayashi, J., Liu, C., Akamatsu, F., Nishiyama, A., Moon, A., & Ikeda, Y. (2017). Effects of Microwave-Enhanced Plasma on Laser Ignition. *Ignition Systems for Gasoline Engines* (pp. 245–253). Springer International Publishing.

Ikeda, Y., Hirata, Y., Soriano, J. K., & Wakaida, I. (2022). Antenna Characteristics of Helical Coil with 2.45 GHz Semiconductor Microwave for Microwave-Enhanced Laser-Induced Breakdown Spectroscopy (MW-LIBS). *Materials*, *15*(8), 2851. Retrieved from https://www.mdpi.com/1996-1944/15/8/2851

Ikeda, Y., Ofosu, J. A., & Wakaida, I. (2020). Development of microwave-enhanced fibre-coupled laser-induced breakdown spectroscopy for nuclear fuel debris screening at Fukushima. *Spectrochimica Acta - Part B Atomic Spectroscopy*, *171*. Elsevier B.V.

Ikeda, Y., Soriano, ; Joey Kim, Ohba, H., & Ikuo, W. (2023a). *Measurement of Uranium Isotope Emission Ratio for Enrichment Level Determination via Microwave-Enhanced Laser-Induced Breakdown Spectroscopy*.

Ikeda, Y., & Soriano, J. K. (2022). Microwave-enhanced laser-induced air plasma at atmospheric pressure. *Optics Express*, *30*(19), 33756. Optica Publishing Group.

Ikeda, Y., & Soriano, J. K. (2023). Analysis of the characteristics of microwave-enhanced laser-induced atmospheric air plasma and ablation plasma for Al target. *Talanta Open*, *7*, 100172.

Ikeda, Y., Soriano, J. K., Akaoka, K., & Wakaida, I. (2023b). Plasma ion emission enhancements of Zr using microwave-enhanced laser-induced breakdown spectroscopy. *Spectrochimica Acta Part B: Atomic Spectroscopy*, *203*, 106651.

Ikeda, Y., Soriano, J. K., Kawahara, N., & Wakaida, I. (2022). Spatially and temporally resolved plasma formation on alumina target in microwave-enhanced laser-induced breakdown spectroscopy. *Spectrochimica Acta Part B: Atomic Spectroscopy*, *197*, 106533. Elsevier. Retrieved October 7, 2022, from https://linkinghub.elsevier.com/retrieve/pii/S058485472200177X

Ikeda, Y., Soriano, J. K., Ohba, H., & Ikuo, W. (2023c). *Laser air plasma expansion by microwaves*.

Ikeda, Y., Soriano, J. K., Ohba, H., & Wakaida, I. (2023d). Laser ablation plasma expansion using microwaves. *Scientific Reports*, *13*(1), 13901.

Ikeda, Y., Soriano, J. K., Ohba, H., & Wakaida, I. (2023e). Analysis of gadolinium oxide using microwave-enhanced fiber-coupled micro-laser-induced breakdown spectroscopy. *Scientific Report*, *13*(4828).

Ikeda, Y., Soriano, J. K., & Wakaida, I. (2022). Signal-to-noise ratio improvements in microwave-assisted laser-induced breakdown spectroscopy. *Talanta Open*, *6*. Elsevier B.V.

Ikeda, Y., Soriano, J. K., & Wakaida, I. (2023a). The interactions of microwaves with alumina surface in microwave-enhanced laser-induced breakdown spectroscopy. *Optics & Laser Technology*, *159*, 108982.

Ikeda, Y., Soriano, J. K., & Wakaida, I. (2023b). Plasma emission intensity expansion of Zr metal and Zr oxide via microwave enhancement laser-induced breakdown spectroscopy. *Journal of Analytical Atomic Spectrometry*.

Ikeda Yuji, Soriano Joey Kim, & Wakaida Ikuo. (2023). Microwave-enhanced laser-induced breakdown spectroscopy of Zirconium metal. *Talanta Open*, *7*(100182).

Karino, T., Akaoka, K., Ohba, H., Wakaida, I., Soriano, J. K., & Ikeda, Y. (2023). Uranium isotope measurement by microwave-enhanced LIBS. *The 5th Asian Symposium on Laser Induced Breakdown Spectroscopy*. Japan.

Kawahara, N., Beduneau, J. L., Nakayama, T., Tomita, E., & Ikeda, Y. (2007). Spatially, temporally, and spectrally resolved measurement of laser-induced plasma in air. *Applied Physics B: Lasers and Optics*, *86*(4), 605–614.

Khumaeni, A., Akaoka, K., Miyabe, M., & Wakaida, I. (2021). The role of metastable atoms in atomic excitation process of magnesium in microwave-assisted laser plasma. *Optics Communications*, *479*. Elsevier B.V.

Khumaeni, A., Miyabe, M., Akaoka, K., & Wakaida, I. (2017). The effect of ambient gas on measurements with microwave-assisted laser-induced plasmas in MA-LIBS with relevance for the analysis of nuclear fuel. *Journal of Radioanalytical and Nuclear Chemistry*, *311*(1), 77–84. Springer Netherlands.

Khumaeni, A., Motonobu, T., Katsuaki, A., Masabumi, M., & Ikuo, W. (2013). Enhancement of LIBS emission using antenna-coupled microwave. *Optics Express*, *21*(24), 29755. The Optical Society.

Le, M. K., Padala, S., Nishiyama, A., & Ikeda, Y. (2017). Control of Microwave Plasma for Ignition Enhancement Using Microwave Discharge Igniter. *SAE Technical Papers* (Vol. 2017-September). SAE International.

Li, C., Guo, L., He, X., Hao, Z., Li, X., Shen, M., Zeng, X., et al. (2014a). Element dependence of enhancement in optics emission from laser-induced plasma under spatial confinement. *Journal of Analytical Atomic Spectrometry*, *29*(4), 638.

Li, C., Guo, L., He, X., Hao, Z., Li, X., Shen, M., Zeng, X., et al. (2014b). Element dependence of enhancement in optics emission from laser-induced plasma under spatial confinement. *Journal of Analytical Atomic Spectrometry*, *29*(4), 638.

Li, H., Mazzei, L., Wallis, C. D., Davari, S. A., & Wexler, A. S. (2021). The performance of an inexpensive spark-induced breakdown spectroscopy instrument for near real-time analysis of toxic metal particles. *Atmospheric Environment*, *264*, 118666. Pergamon.

Liu, Y., Baudelet, M., & Richardson, M. (2010). Elemental analysis by microwave-assisted laser-induced breakdown spectroscopy: Evaluation on ceramics. *Journal of Analytical Atomic Spectrometry*, *25*(8), 1316.

Liu, Y., Bousquet, B., Baudelet, M., & Richardson, M. (2012). Improvement of the sensitivity for the measurement of copper concentrations in soil by microwave-assisted laser-induced breakdown spectroscopy. *Spectrochimica Acta - Part B Atomic Spectroscopy*, *73*, 89–92.

Nakanishi, R., Saeki, M., Wakaida, I., & Ohba, H. (2020). Detection of Gadolinium in Surrogate Nuclear Fuel Debris Using Fiber-Optic Laser-Induced Breakdown Spectroscopy under Gamma Irradiation. *Applied Sciences*, *10*(24), 8985.

Pedarnig, J. D., Haslinger, M. J., Bodea, M. A., Huber, N., Wolfmeir, H., & Heitz, J. (2014). Sensitive detection of chlorine in iron oxide by single pulse and dual pulse laser-induced breakdown spectroscopy. *Spectrochimica Acta Part B: Atomic Spectroscopy*, *101*, 183–190. Retrieved from https://www.sciencedirect.com/science/article/pii/S0584854714002031

Qi, J., Zhang, T., Tang, H., & Li, H. (2018). Rapid classification of archaeological ceramics via laser-induced breakdown spectroscopy coupled with random forest. *Spectrochimica Acta - Part B Atomic Spectroscopy*, *149*, 288–293. Elsevier B.V.

Rai, V. N., & Thakur, S. N. (2020). Instrumentation for LIBS and recent advances. *Laser-Induced Breakdown Spectroscopy*, 107–136. Elsevier.

Rohwetter, P., Yu, J., Méjean, G., Stelmaszczyk, K., Salmon, E., Kasparian, J., Wolf, J. P., et al. (2004). Remote LIBS with ultrashort pulses: Characteristics in picosecond and femtosecond regimes. *Journal of Analytical Atomic Spectrometry* (Vol. 19, pp. 437–444).

Ruas, A., Matsumoto, A., Ohba, H., Akaoka, K., & Wakaida, I. (2017). Application of laser-induced breakdown spectroscopy to zirconium in aqueous solution. *Spectrochimica Acta - Part B Atomic Spectroscopy*, *131*, 99–106. Elsevier B.V.

Al Shuaili, A. A., Al Hadhrami, A. M., Wakil, M. A., & Alwahabi, Z. T. (2019). Improvement of palladium limit of detection by microwave-assisted laser induced breakdown spectroscopy. *Spectrochimica Acta - Part B Atomic Spectroscopy*, *159*. Elsevier B.V.

Tampo, M., Miyabe, M., Akaoka, K., Oba, M., Ohba, H., Maruyama, Y., & Wakaida, I. (2014). Enhancement of intensity in microwave-assisted laser-induced breakdown spectroscopy for remote analysis of nuclear fuel recycling. *J. Anal. At. Spectrom.*, *29*(5), 886–892.

Tang, Y., Li, J., Hao, Z., Tang, S., Zhu, Z., Guo, L., Li, X., et al. (2018). Multielemental self-absorption reduction in laser-induced breakdown spectroscopy by using microwave-assisted excitation. *Optics Express*, *26*(9), 12121. The Optical Society.

Thakur, S. N., & Singh, J. P. (2020). Fundamentals of LIBS and recent developments. *Laser-Induced Breakdown Spectroscopy*, 3–22. Elsevier.

Viljanen, J., Zhao, H., Zhang, Z., Toivonen, J., & Alwahabi, Z. T. (2018). Real-time release of Na, K and Ca during thermal conversion of biomass using quantitative microwave-assisted laser-induced breakdown spectroscopy. *Spectrochimica Acta - Part B Atomic Spectroscopy*, *149*, 76–83. Elsevier B.V.

Viljanen, Jan, Sun, Z., & Alwahabi, Z. T. (2016). Microwave assisted laser-induced breakdown spectroscopy at ambient conditions. *Spectrochimica Acta - Part B Atomic Spectroscopy*, *118*, 29–36. Elsevier B.V.

Wolk, B., DeFilippo, A., Chen, J. Y., Dibble, R., Nishiyama, A., & Ikeda, Y. (2013). Enhancement of flame development by microwave-assisted spark ignition in constant volume combustion chamber. *Combustion and Flame*, *160*(7), 1225–1234.

Zhang, Z., Wu, J., Hang, Y., Zhou, Y., Tang, Z., Shi, M., Qiu, Y., et al. (2022). Quantitative analysis of chlorine in cement pastes based on collinear dual-pulse laser-induced breakdown spectroscopy. *Spectrochimica Acta Part B: Atomic Spectroscopy*, *191*, 106392. Retrieved from https://www.sciencedirect.com/science/article/pii/S0584854722000362